Assessing the impacts of sedimentation settings in double-moment microphysical schemes on the kinematic-thermodynamic characteristics of nocturnal convective systems

Frederick Iat-Hin Tam (譚日軒)[1], Ming-Jen Yang (楊明仁)[1], Wen-Chau Lee[2]

[1]Department of Atmospheric Sciences, National Taiwan University, Taipei, Taiwan
[2]National Center for Atmospheric Research, Boulder, Colorado, USA

Abstract

In this study, numerical simulations of a nocturnal mesoscale convective system (MCS) during the 2015 Plains Elevated Convection at Night (PECAN) field campaign were used to gauge the impacts of hydrometeor sedimentation settings in double-moment microphysical schemes on these MCSs. The simulation results indicate that differential sedimentation of rimed particles could potentially yield the greatest impact on the simulated MCSs, namely intensifying their updrafts at the middle levels. This mid-level updraft intensification is shown to be accompanied with more intense system mid-level rear-to-front (RTF) inflows.

Through analyzing the rimed particle size statistics and pressure perturbation for simulations with more intense mid-level updrafts, we found that preferential fallout of larger particles near the MCS system edge could generate more robust negative pressure perturbation near the updrafts through graupel melting. The pressure gradient force associated with this anomaly could potentially enhance the RTF inflow. Stronger RTF inflows might intensify updrafts since they (i) limited the updraft tilt, and (ii) allowed shed water drops to refreeze in the system updrafts. We further found that disabling this kinematic-thermodynamic feedback could decrease the riming heating aloft by up to 46%. Lastly, comparing the RTF inflow characteristics in simulations with different rimed particle size-terminal velocity relationships confirms the criticalness of rimed particle sedimentation near system edge in determining the strength and extent of the simulated MCS's RTF inflow.

Keywords: Mesoscale Convective Systems; RTF inflows; Microphysical Parameterizations; Hydrometeor Sedimentation.

1. Introduction

The use of more sophisticated model parameterization schemes in practical and research settings is increasingly common as computational resources become more affordable. A rationale to justify the use of these schemes is that they might depict different weather phenomena in a more realistic manner. For example, the utilization of multi-moment (MM) microphysical schemes has been shown to yield tangible improvements over single-moment (SM) alternatives on precipitation intensity and storm structure (e.g. van Weverberg et al. 2012; Molthan and Colle 2012; Yussouf et al. 2013; Putnam et al. 2017).

One of the potential advantages of MM microphysical parameterization schemes is their abilities to realistically represent hydrometeor sedimentation. This is accomplished by allowing hydrometeor moments to fallout at their uniquely weighted terminal velocities (Mansell 2010). MM schemes are, therefore, capable of representing processes like size sorting, which had hitherto been unable to reproduce with SM schemes.

There are two main possible avenue with which hydrometeor sedimentation could impact convective systems. The first of which is via cold pool-related low-level lifting. Dawson et al. (2010) found that rainwater size sorting in MM schemes could partially alleviate the well-known cold bias in SM simulations of cold pools via better treatment of rain drop size distribution (DSD) and evaporation; this could feedback upon simulated storm intensity through better realized low-level lifting. The second of which is related to mid-level circulation intensity. Changing the prescribed rimed particle properties in SM schemes has been shown to change the system rear inflow and updraft at the middle levels (e.g., Yang and Houze 1995; Adams-Selin et al. 2013; Siegel and van den Heever 2013). To the authors' best knowledge, however, there has been relatively few attempts to isolate the impact of hydrometeor sedimentation on the mid-level circulations with MM schemes.

In this study, we attempt to quantify this impact with multiple microphysical sensitivity experiments with different parameterized sedimentation settings on a nocturnal convective system. The results provide therein will indicate a correlation between rimed particle sedimentation and mid-level circulations, mainly through controlling the latent cooling and associated buoyancy forcing near the melting level.

2. Methodology

a) Changing sedimentation settings

Results from two sets of sensitivity experiments will be presented therein. In the first simulation set, we test the role of size sorting by alternatively disabling the differential fallout of

different hydrometeor types during sedimentation. To disable size sorting, we force the two predicted hydrometeor moments to fallout at the same terminal velocity, which will essentially eliminate the vertical evolution of hydrometeor mean mass diameter (Mansell 2010). In the second group of simulations, we multiply the parameterized terminal velocity-diameter power law relationship for graupel:

$$V_{tg} = \left(\frac{1{,}204}{\rho_{air}}\right)^{0.5} \frac{4\rho_g g}{3C_D\rho_{air}} D^{0.5} \quad (1),$$

by a factor ranging from 0.25 to 3.0. The goal of this adjustment is to quantify the responses of simulated convective systems to a steadily increasing sedimentation rate.

b) Dynamical diagnostic framework

We examine the impact of sedimentation on mid-level circulations by considering the following diagnostic Poisson equation of total pressure perturbation (P') from the momentum equations of an inviscid, anelastic Boussinesq flow system:

$$\nabla^2 P' = \nabla^2 P'_D + \nabla^2 P'_B = -\nabla \cdot \left(\rho\vec{V} \cdot \nabla\vec{V}\right) + \frac{\partial \rho B}{\partial z} \quad (2),$$

with the first and second terms of the right hand side representing the dynamic and buoyancy contributions to the pressure perturbation field, respectively. The contributions of these pressure anomalies to the storm circulation can then be estimated by their corresponding pressure gradient force.

3. Results

a) System-scale responses to the varied sedimentation scenarios

Our initial analysis concerns the impact of sedimentation on accumulated surface precipitation. The 2-h mature phase accumulated precipitation probability distribution functions (PDFs; Fig. 1) reveals large variances in the precipitation statistics, suggesting a non-trivial role for hydrometeor sedimentation. We find that the precipitation PDFs deviate from the FULL simulation most strongly either when graupel size sorting is turned off, or when the graupel terminal velocity is artificially lowered by the imposed factor. The system severe precipitation potential is shown to be substantially lowered with these sedimentation settings. On the other hand, the impacts of disabling the size sorting for other hydrometeor type and increasing the graupel terminal velocity are rather slight, with only minor differences from the FULL PDF.

The kinematic responses of simulated MCSs to sedimentation settings can be elucidated from the mean and 10th-90th percentile updrafts and downdrafts profiles (Fig. 2). The simulations that exhibit the largest negative deviation from FULL in precipitation generally contain weaker updrafts than the other simulations. The graupel mixing ratios of these simulations are also smaller (not shown), which points to less vigorous mixed phase particle production in these systems. The difference between the FULL and disable graupel size sorting simulation (GNSS) in graupel mass reaches 80% at 4 km. Graupel terminal velocity-diameter power laws are also shown to exert influence on the system kinematics, with smaller (larger) *Vtg* resulting in weaker (stronger) updrafts. Updraft enhancements for increase-*Vtg* simulations are centered above 6 km and are associated with increased production of low-density snow and ice (not shown). Inability of these particles to fallout beneath the melting level might be a reason for the similarity between the PDFs for these simulations and the FULL PDF.

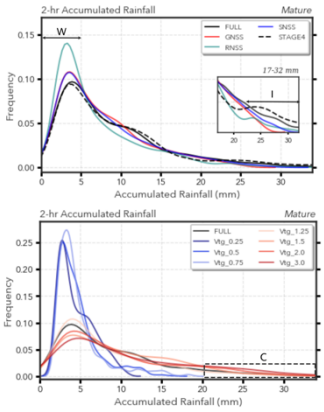

Figure 1: Probability density functions (PDFs) of the simulated 2-h accumulated rainfall during mature phase for (upper) size sorting and (lower) *Vtg* experiments.

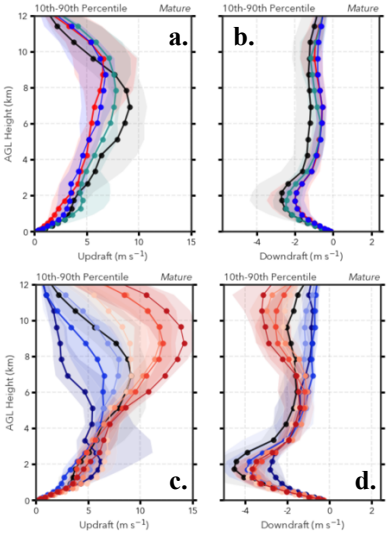

Figure 2: Mean (lines) and 10th-90th percentile mature phase updrafts (left column) and downdrafts (right column) for the (upper row) size sorting and (lower row) *Vtg* experiments.

b) Thermodynamic and circulation sensitivities

We now review the changes in MCSs' thermodynamic and circulation features that are related to the different sedimentation settings. For brevity, only a portion of the results with the most critical findings will be shown therein.

By comparing the line-averaged system-relative wind structures (Fig. 3), we find that MCSs that are kinematically stronger (Fig. 3a, b) tend to exhibit circulation structures that are more consistent with the schematic diagram for mid-latitude squall lines by Houze et al. (1989). Specifically, these MCSs contain relatively upright ascending front-to-rear (FTR) flows and strong mid-level rear-to-front (RTF) inflows. The kinematically weaker MCSs (Fig. 3c,d), on the other hand, contain RTF inflows that are weaker and descend earlier than stronger MCSs. Stronger mid-level rear inflows can neutralize the deep layer environmental shear and limit the updraft tilt. We note that our results are consistent with the SM study by Siegel and van den Heever (2013), which suggests a coherent response of rear inflows to hail mean diameters in prescribed hail DSDs. This also means that we could possibly attribute the circulation changes in Fig. 3 to the differential graupel fallout in the simulated MCSs.

The thermodynamic characteristics of stronger and weaker MCSs (Fig. 3) can be differentiated with two main factors: Firstly, net latent heating rates in the weaker MCSs' updrafts are generally weaker. Comparing the individual heating components terms suggest that MCSs with more net heating tend to have deeper and stronger riming heating above the melting level, and vice versa. Secondly, we find that the latent cooling of the stronger MCSs generally have deeper and more intense cooling; they are also more concentrated to the MCSs' edge than weaker MCSs, which have more uniformly-distributed latent cooling.

To quantify the impact of different sedimentation settings on MCS thermodynamics, we integrate the individual latent heating/cooling components with height and compare the relative differences of simulations shown in Fig. 3 to the FULL (Table 1). Riming and melting are shown to be the terms that respond most similarly to sedimentation settings as net heating/cooling. This affirms the role of the production of heavier rimed particles and their subsequent fallout in adjusting the thermodynamic structures of the simulated MCSs.

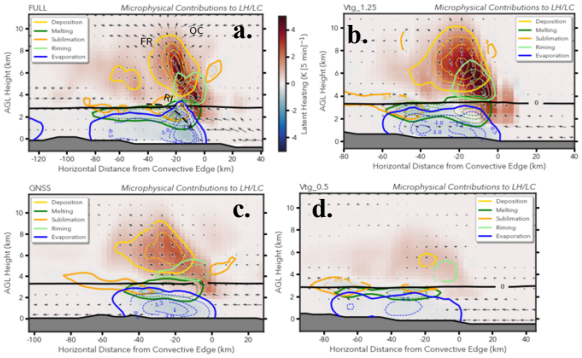

Figure 3: Net latent heating rate (color) and latent heating/cooling contributions from different microphysical processes (contours). Shown in this figure are the results from the (a) FULL, (b) Vtg_1.25, (c) GNSS, and (d) Vtg_0.5, respectively.

Process \ Experiment	FULL	GNSS	Vtg_1.25	Vtg_0.5
Net LH	2.29	1.95 (-14.9%)	2.75 (+20.1%)	1.56 (-31.9%)
Deposition	4.40	4.32 (-2.0%)	4.70 (+6.8%)	3.14 (-28.6%)
Riming	0.38	0.21 (-46.1%)	0.39 (+2.6%)	0.23 (-39.5%)
Sublimation	-2.08	-1.80 (-13.3%)	-1.90 (-8.7%)	-1.47 (-29.3%)
Melting	-0.39	-0.33 (-15.2%)	-0.40 (+2.6%)	-0.30 (-23.1%)
Evaporation	-1.19	-1.04 (-12.1%)	-1.21 (+1.7%)	-1.15 (-3.4%)

Table 1. Integrated latent heating and cooling rates for (left to right) the FULL, GNSS, Vtg_1.25, Vtg_0.5, respectively. Percentages in parentheses are the relative differences of each simulations to the corresponding FULL values.

c) Dynamic inferences

To find a link between the identified thermodynamic and kinematic sensitivities, we derived the pressure perturbation components for two stronger and two weaker MCSs. Figure 4 shows the line-averaged buoyancy component. We will focus on the buoyancy contributions in this section because they are much larger than the dynamic contributions for all simulations (not shown).

For the stronger MCSs (Fig. 4a,b; Fig.5a,b), a negative anomaly in buoyancy pressure perturbation (P_B') can be identified near the MCS edge, beneath the updrafts. The locations of these MCSs' negative P_B' is consistent with the enhanced vertical buoyancy gradient (not shown) associated

with their concentrated latent cooling (Fig. 3). In contrast, the negative P_B' anomalies of the weaker MCSs (Fig. 4c,d) are generally weaker and less concentrated to the MCS edge. For certain sedimentation settings (i.e. Vtg_0.5; Fig. 4d), we identify a second weak negative P_B' anomaly in the rear of the MCS.

To provide further evidence to the purported thermodynamic and kinematic sensitivities, we calculated the pressure gradient force associated with the derived buoyancy pressure perturbation (Fig. 5). The strong and concentrated negative P_B' anomaly created an area with enhanced rear-to-front flow forcing behind the updrafts. For the weaker MCSs, comparable rear-to-front forcing are located further away from the updrafts. This result is significant because it related the thermodynamic responses to sedimentation settings, i.e. concentration of latent cooling, to the kinematic and circulation responses discussed in previous sections. Specifically, we show that sedimentation settings of graupel particles could meaningfully impact the strength and extent of mid-level rear-to-front inflow.

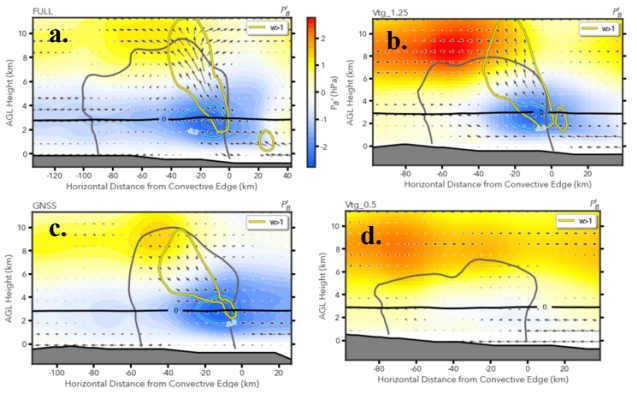

Figure 4: P_B' (color) and 1 m s^{-1} vertical velocity (yellow contours). Shown in this figure are the results from the (a) FULL, (b) Vtg_1.25, (c) GNSS, and (d) Vtg_0.5, respectively.

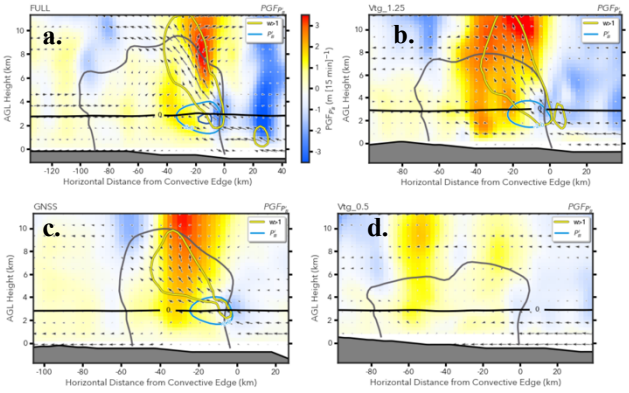

Figure 5: Same as Figure 4, but for the pressure gradient force associated with P_B' (color).

4. Conclusions

A series of simulations on a nocturnal MCS were conducted to understand the impact of sedimentation settings in MM microphysical parameterization schemes on MCS intensity and precipitation potential. The simulation results indicate that graupel, despite it not being the most dominant hydrometeor type aloft, yields the greatest impacts on MCS kinematic and thermodynamic structures. This outsized influence is primarily due to the closeness of graupel formation area to the melting level and the rather large V_{tg}, both of which would make the mid-level kinematic and thermodynamic features susceptible to adjustments in graupel characteristics.

The primary statistical insights include: (1) Reduced severe precipitation potential for sedimentation settings that restrict the fallout of heavier rimed particles. (2) Increased severe precipitation potential in certain sedimentation settings is correlated to stronger system-scale mid-level updraft strength in these simulations.

A physical explanation is presented with cross-section and dynamic diagnostical analysis to interpret the above statistical findings. It is found that MCSs with stronger mid-level updrafts can be dynamically distinguished from weaker MCSs with weaker/less extended mid-level rear inflow and increased rearward tilt of MCS updrafts. Increased updraft tilt reduces the amount of supercooled droplets aloft, thus results in less effective riming growth.

The dynamical feature most sensitive to the rimed particle sedimentation settings is mid-level rear inflows. Sedimentation setting that leads to less effective graupel fallout produce less rimed particles and are much less efficient in letting these hydrometeors to fall beneath the melting level. As a result, the MCS latent cooling will be weakened and shift slightly to the system rear. As demonstrated by the pressure perturbation diagnostical model, sedimentation-related impacts on the MCS thermodynamics lead to less apparent negative P_B' and rear-to-front flow forcing near the edge of the MCS. Settings that enhance the effectiveness of rimed particle fallout, on the other hand, produces stronger negative P_B' and stronger mid-level rear inflows.

In general, our results add to an emerging consensus of the benefit of using MM microphysical schemes in convective-permitting forecasts (e.g. Yussouf et al. 2013; Igel et al. 2015; Putnam et al. 2017). A particularly relevant finding from our results is that rimed particle sedimentation settings could introduce substantial variances to model performance on nocturnal MCSs. This indicates that future research into improving the treatment of particle sedimentation in models could potentially lower forecast bias for such systems and should be encouraged.

5. References

Adams-Selin, R.D., S.C. van den Heever, and R.H. Johnson, 2013a: Impact of Graupel Parameterization Schemes on Idealized Bow Echo Simulations. *Mon. Wea. Rev.*, **141**, 1241–1262.

Dawson, D. T., M. Xue, J. A. Milbrandt, and M. K. Yau, 2010: Comparison of evaporation and cold pool development between single-moment and multimoment bulk microphysics schemes in idealized simulations of tornadic thunderstorms. *Mon. Wea. Rev.*, **138**, 1152–1171.

Igel, A.L., M.R. Igel, and S.C. van den Heever, 2015: Make It a Double? Sobering Results from Simulations Using Single-Moment Microphysics Schemes. *J. Atmos. Sci.*, **72**, 910–925.

Houze, R. A., Jr., 1989: Observed structure of mesoscale convective systems and implications for large-scale heating. *Quart. J. Roy. Meteor. Soc.*, **115**, 425-461.

Mansell, E.R., 2010: On Sedimentation and Advection in Multimoment Bulk Microphysics. J. Atmos. Sci., 67, 3084–3094.

Molthan, A.L. and B.A. Colle, 2012: Comparisons of Single- and Double-Moment Microphysics Schemes in the Simulation of a Synoptic-Scale Snowfall Event. *Mon. Wea. Rev.*, **140**, 2982–3002.

Putnam, B. J., M. Xue, Y. Jung, N. A. Snook, and G. Zhang, 2017: Ensemble Probabilistic Prediction of a Mesoscale Convective System and Associated Polarimetric Radar Variables Using Single-Moment and Double-Moment Microphysics Schemes and EnKF Radar Data Assimilation. *Mon. Wea. Rev.*, **145**, 2257–2279.

Seigel, R.B. and S.C. van den Heever, 2013: Squall-Line Intensification via Hydrometeor Recirculation. *J. Atmos. Sci.*, **70**, 2012–2031.

van Weverberg, K., A.M. Vogelmann, H. Morrison, and J.A. Milbrandt, 2012: Sensitivity of Idealized Squall-Line Simulations to the Level of Complexity Used in Two-Moment Bulk Microphysics Schemes. *Mon. Wea. Rev.*, **140**, 1883–1907.

Yang, M. and R.A. Houze, 1995: Sensitivity of Squall-Line Rear Inflow to Ice Microphysics and Environmental Humidity. *Mon. Wea. Rev.*, **123**, 3175–3193.

Yussouf, N., E. R. Mansell, L. J. Wicker, D. M. Wheatley, and D. J. Stensrud, 2013: The Ensemble Kalman Filter Analyses and Forecasts of the 8 May 2003 Oklahoma City Tornadic Supercell Storm Using Single- and Double-Moment Microphysics Schemes. *Mon. Wea. Rev.*, **141**, 3388.